ELSEVIER

Continuous sample rotation data collection for protein crystallography with the PILATUS detector

Ch. Brönnimann[a,*], E.F. Eikenberry, R. Horisberger[b], G. Hülsen[a], B. Schmitt[a],
C. Schulze-Briese[a], T. Tomizaki[a]

[a] Swiss Light Source (SLS), WSLA/218, Paul Scherrer Institute, CH-5232 Villigen, Switzerland
[b] Paul Scherrer Institute, CH-5232 Villigen, Switzerland

Abstract

The PILATUS detector (pixel apparatus for the SLS) is a large all silicon quantum-limited area X-ray detector for protein crystallography. A three-module array with 1120×157 pixels covering an active area of $24.3 \times 3.6 \, cm^2$ is in operation. Its main features are an excellent point-spread function, a very high dynamic range and a readout time of $< 7 \, ms$. X-rays with energy above 6 keV can be detected in single photon counting mode. To demonstrate the potential of the detector, fine ϕ-sliced protein crystal data were collected in continuous sample rotation mode at beamline X06SA of the SLS.

© 2003 Elsevier B.V. All rights reserved.

Keywords: Protein crystallography; Single-photon counting; Fine ϕ-slicing; Continuous sample rotation

1. Introduction

The first fully operational beamline of the Swiss Light Source (SLS) is the protein crystallography beamline X06SA. High brightness synchrotron radiation in the 1 Å wavelength regime is produced by an in-vacuum minigap undulator. A dynamically focused optical system adjusts the beam to the sample. This enables the study of biological crystals with small physical dimensions. Another key component of the beamline is the fast framing pixel detector for high-resolution data-acquisition, which is described.

The basic setup for crystallography experiments is shown diagrammatically in Fig. 1. The crystal is frequently cooled by a cryogenic gas stream to increase its lifetime with respect to X-ray beam damage. The crystal is rotated about the ϕ-axis spindle by means of a goniometer. The resulting two-dimensional diffraction patterns as a function of rotation angle are recorded by the detector.

The principal requirements of the detector are as follows: The detector should have high counting capacity to record the diffracted rays, which can produce count rates of up to 10^6 X-ray/s. Very weak reflections must be recorded simultaneously. Therefore, a high dynamic range is needed, preferably greater than 3×10^4. The detector must have a very good point spread function. In addition, a high detective quantum efficiency (DQE) is required. Other important parameters,

*Corresponding author. Tel.: +41-56-310-3764; fax: +41-56-310-3151.

E-mail address: christian.broennimann@psi.ch
(C. Brönnimann).
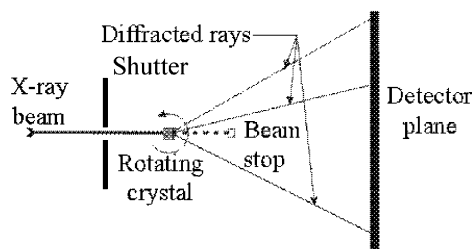
Fig. 1. Experimental setup for macromolecular crystallography. The X-ray beam from a synchrotron impinges on a crystal held in a thin-walled capillary or in a frozen drop. A shutter is used to synchronize the exposure with the detector. The crystal is rotated about the ϕ-axis to produce diffraction patterns recorded by the detector as a function of rotation angle. The beamstop for the direct beam is indicated.

which will be described in more detail in the next section are the readout time and the frame rate of the detector. The new generation of detectors for protein crystallography should have readout times in the ms-range and frame rates of the order of 10 Hz.

Detector types, which fulfill almost all of these requirements, are hybrid pixel detectors operated in single photon counting mode [1–3]. Due to the direct detection of the X-rays with a silicon sensor, the point-spread function of such detectors is excellent. The DQE is given by the absorption of the X-rays by the silicon, which is 75% at 12 keV for a 0.3 mm thick sensor. One of the most advanced systems is the three module-array of the PILATUS detector. The principle and the specifications of the full detector are described in Ref. [4].

2. "Traditional" and fine ϕ-sliced data collection

The "traditional" way of data collection for protein crystallography is the following:

After aligning the crystal in the beam, some test shots are performed to determine the quality of the crystal.

Based on these results, the rotation angle per frame, the integration time per frame, and the total rotation angle are determined. Now the actual measurement starts. With the shutter closed, the

ϕ-axis is accelerated, the shutter being opened at the end of the acceleration phase. For the preset integration time, the crystal is rotated with constant angular velocity. After the shutter is closed, the crystal is decelerated and rotated back to the starting point for the next frame, while the detector is read out. It is clear that this method imposes high requirements on the precision of the synchronization between the goniometer and the shutter system. Typical parameters at the beamline X06SA are integration times of 0.5–60 s and rotation angles of 0.5–1°/frame. As an example, the readout time of the commercial detector at the beamline is 2.5 s.

A desired mode of data collection is fine ϕ-slicing, preferred because it has the potential to improve the signal-to-noise ratio (SNR) of the Bragg reflections (diffraction maxima) as shown by theoretical modeling, buttressed by some experimental data [5,6]. In this mode the crystal is rotated by a fraction of its angular acceptance (0.02–0.2°) during each frame, leading to data sets of as many as 9000 frames for a full 180° rotation. Clearly, such an experiment is very time consuming with a commercial detector. With a fast framing detector the crystal can be rotated *continuously* in the beam without opening and closing the shutter for each frame. For such an experiment, an electronically gateable detector is needed, because of the absence of the mechanical shutter. Since the crystal is rotated without any shutter operation, the readout time of the detector needs to be as fast as possible, in order to reduce the dead-time during the rotation of the crystal. And, most important, the detector should not add any additional noise to the data, when being read out.

The fine-ϕ-slicing method utilizes the same total X-ray dose to the crystal, but has the following advantages:

- It optimizes the SNR of the Bragg reflections.
- It requires only minimal synchronization between shutter, goniometer and detector.
- It increases the dynamic range due to over-sampling of the bragg spots. Thus high- and low-resolution data can be obtained in a single data set.

- It may reduce radiation damage to the crystal due to constant dose rate of the crystal in the beam.

To summarize, crystallographic data obtained with continuous fine ϕ-slicing are easier to obtain, and potentially lead to data of superior quality.

3. PILATUS detector architecture

The fundamental unit of the PILATUS detector is the module, consisting of a single fully depleted monolithic silicon sensor $80 \times 36\,\mathrm{mm}^2 \times 300\,\mu\mathrm{m}$ thick (Colybris SA, Neuchatel, Switzerland), bump-bonded to a 2×8 array of readout chips using $17\,\mu\mathrm{m}$ diameter indium balls. The readout chips, fabricated on $15\,\mathrm{cm}$ wafers in the DMILL radiation-tolerant CMOS process (Atmel Temic SA, Nantes, France), are $10 \times 20\,\mathrm{mm}^2$ and contain a 44×78 array of $217 \times 217\,\mu\mathrm{m}^2$ pixels. Bump-bonding was performed with the micro-bump-bonding process developed at PSI.

The sensor is continuous, with no dead area. Double-size pixels are used at the chip boundaries to span the gap between readout chips. The detector operates at room temperature, but is water-cooled because each module dissipates about $10\,\mathrm{W}$.

Each pixel contains a charge-sensitive preamplifier and shaper, a single-level discriminator, and a 15-bit pseudo-random counter. Thus, the data are stored in digital form in the pixel. The amplifier noise is $75\,\mathrm{e}^-$, which permits single-photon counting at energies even below $6\,\mathrm{keV}$ [7]. Each pixel is xy-addressable and contains a 4-bit threshold trim adjustment.

Two modes are defined: The counting mode, in which all pixels individually count incoming X-rays, and the readout mode, in which the stored data may be accessed.

The three-module assembly is shown in Fig. 2. The read out is performed serially at a clock frequency of $10\,\mathrm{MHz}$, and leads to a readout time of $<7\,\mathrm{ms}$ for one chip. Since all chips are read out in parallel, the readout time for the full detector is also $<7\,\mathrm{ms}$. The module control board (MCB)
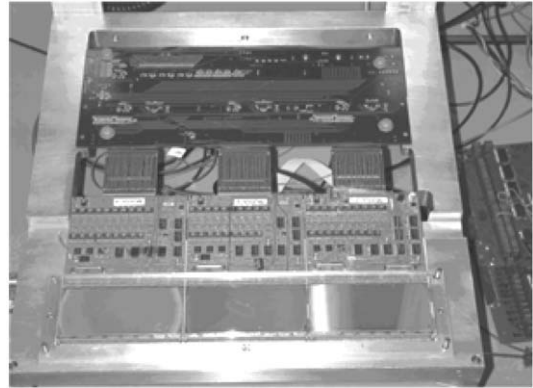
Fig. 2. A bank of three PILATUS flat-type modules, constituting a 1120×157 pixel array. The three sensors, each with 366×157 pixels, are in the foreground. Behind them are three flat MCBs and at the rear is the BCB connected by adapter cards.
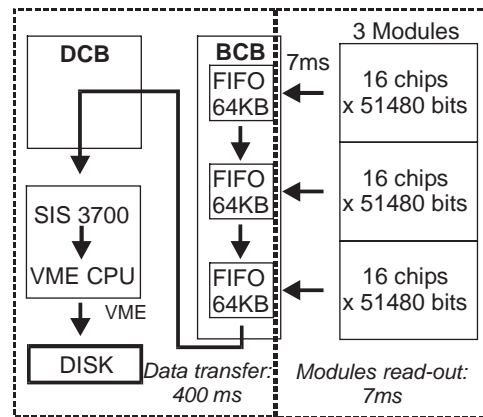
Fig. 3. The readout architecture of the three-module system. Digital data from all the chips are read out in parallel with $10\,\mathrm{MHz}$ and are stored in the FIFOs on the BCB. During the next exposure, the FIFO data are read out via the detector control board (DCB) into an SIS 3700 VME FIFO and from there transferred to disk. This sequence currently takes $400\,\mathrm{ms}$; a faster DAQ system is currently under development.

carries the electronics needed to operate the 2×8 array and provides optical isolation of all signals.

In order to service three modules a bank control board (BCB) is implemented. Its purpose is to store the digital data from the modules, allowing the chips to resume counting, and multiplex the data onto the output bus. The readout architecture, shown in Fig. 3, minimizes the ratio of the

dead-time to the readout time of the chip, and permits the necessary data transfer to disk during the next exposure time. This allows one to minimize the actual dead-time to the readout time of one chip and to perform the necessary data transfer to disk during the next exposure time. During the fine ϕ-slicing experiment at the beamline, the timing was as follows: The crystal rotation was started, the shutter was opened and the acquisition started with a 500 ms integration phase where the detector was in counting mode.

This was followed by a 6.7 ms readout phase, where the digital data were transferred from the readout chips to the FIFOs on the BCB. The corresponding bandwidth was 55 Mbyte/s. During the next 500 ms counting phase, the data stored on the BCB were transferred at a lower bandwidth to a VME module and from there via NFS to disk. The resulting duty cycle was 98.6%.

4. Experimental results

The diffraction data of a frozen crystal of lysozyme were collected in the following way: First, a threshold trim adjustment procedure with a threshold of $\sim$6 keV, described in Ref. [8], was performed. Then the beam was adjusted to 14 keV and flat field data were collected with Br fluorescence X-rays from a KBr sample at 11.9 keV. For this purpose, the detector was positioned at 90° to the beam. For the crystallography experiment the single bank detector was translated vertically to six positions. At each position 500 frames were taken, each with an exposure time of 0.5 s at a rotation speed of 0.04°/s leading to an integration of 0.02°/frame. The crystal was rotated by 10° at each position. In Fig. 4 the average count rate of 25 background pixels not containing Bragg peaks during the 500 frames is plotted. It can be seen that

Fig. 4. Average count rate of 25 pixels in the background of the diffraction pattern. It can be seen that the background is very stable, due to the very precise timing of the continuous sample rotation. The smooth slope is coming from the self-absorption of the crystal during its rotation.
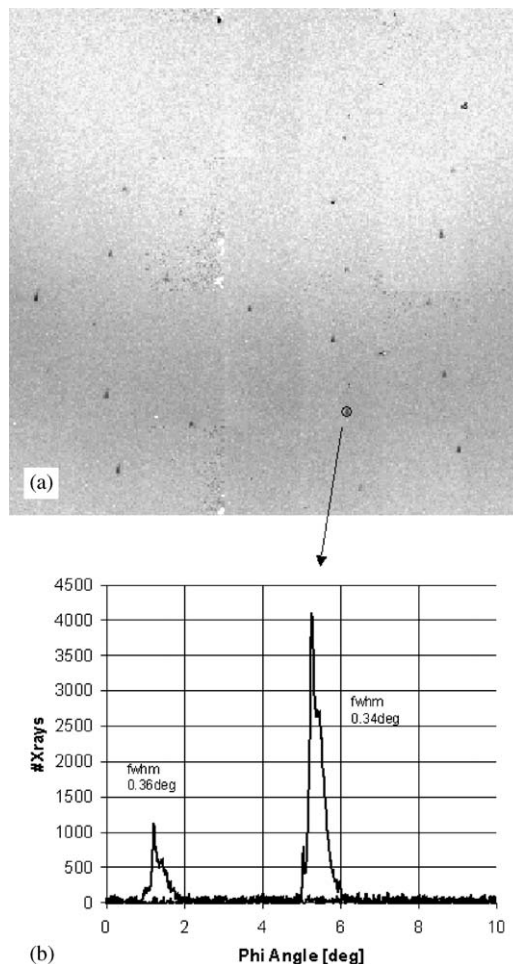
Fig. 5. (a) (top) Section (300 × 300 pixels) of one frame (No. 280, $\phi = 5.6°$) of the fine ϕ-sliced data. Several Bragg diffraction maxima are visible. (b) (bottom) For the marked reflection, the integrated intensity is plotted as a function of the rotation angle. As can be seen, the reflections were heavily oversampled. The mosaicity of the crystal was rather high, leading to broad peaks both in space (top) and in ϕ (bottom).

the background is very constant during the 250 s exposure of the crystal.

In particular, no effect of the top-up injection from the SLS-storage ring is visible, which was done automatically about every 120 s during this experiment.

In Fig. 5a, one frame of the data set is shown with one reflection marked. The integrated number of X-rays is plotted as a function of the rotation angle for the marked reflection and a second one in Fig. 5b. From the profile of the reflections both in Fig. 5a and b, it can be seen that the crystal was rather highly mosaic.

We are currently working on the analysis of these data. Besides the flat-field correction mentioned above, other corrections need to be implemented: A geometrical correction is required to adjust the relative positions of the three modules to each other. (The precision of pixels within a module is defined by very precise photolithographic processes.) Parallax correction will also be applied to the data; X-rays impinging on the sensor at non-normal angles have a significant probability to be converted in a neighboring pixel.

In addition, dead-time correction needs to be implemented to take into account the non-negligible dead-time of the amplifier-counter system. Studies of the detector have shown that during the data-taking phase, the average dead-time of the counter was about 400 ns. In order to obtain accurately the integrated intensities of the diffraction peaks, the data need to be corrected for this effect.

References

[1] C. Schwarz, M. Campbell, R. Goeppert, E.H.M. Heijne, J. Ludwig, G. Meddeler, B. Mikulec, E. Pernigotti, M. Rogalla, K. Runge, A. Soldner-Rembold, K.M. Smith, W. Snoeys, J. Watt, Nucl. Phys. B 78 (1999) 491.

[2] P. Datte, A. Birkbeck, E. Beauville, F. Druillole, L. Luo, J. Millaud, H.H. Xuong, Nucl. Instr. and Meth. A 421 (1999) 576.

[3] M.S. Passmore, R. Bates, K. Mathieson, V. O'Shea, M. Rahman, P. Seller, K.M. Smith, Nucl. Instr. and Meth. A 466 (2001) 202.

[4] Ch. Brönnimann, R. Baur, E.F. Eikenberry, P. Fischer, S. Florin, R. Horisberger, M. Lindner, B. Schmitt, C. Schulze, Nucl. Instr. and Meth. A 477 (2002) 531.

[5] W. Kabsch, International tables for crystallography, in: M.G. Rossmann, E. Arnold (Eds.), Crystallography of Biological Macromolecules, Vol. F, Kluwer Academic Publishers, Dordrecht, 2001 (Chapter 11.3).

[6] J.W. Pflugrath, Acta Crystallogr. D 55 (1999) 1718.

[7] Ch. Brönnimann, R. Baur, E.F. Eikenberry, S. Kohout, M. Lindner, B. Schmitt, R. Horisberger, Nucl. Instr. and Meth. A 465 (2001) 235.

[8] E.F. Eikenberry, Ch. Brönnimann, G. Hülsen, H. Toyokawa, R. Horisberger, B. Schmitt, C. Schulze-Briese, T. Tomizaki, Nucl. Instr. and Meth. A 501 (2003) 260.